Urban Climate 37 (2021) 100868

Contents lists available at ScienceDirect

Urban Climate

journal homepage: www.elsevier.com/locate/uclim

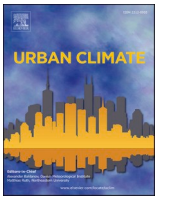

Coupling traffic originated urban air pollution estimation with an atmospheric chemistry model

Attila Kovács [a], Ádám Leelőssy [a,*], Tamás Tettamanti [b], Domokos Esztergár-Kiss [c], Róbert Mészáros [a], István Lagzi [d]

[a] Department of Meteorology, Eötvös Loránd University, 1117 Pázmány Péter sétány 1/A., Budapest, Hungary
[b] Department of Control for Transportation and Vehicle Systems, Faculty of Transportation Engineering and Vehicle Engineering, Budapest University of Technology and Economics, 1111 Műegyetem rkp. 3., Budapest, Hungary
[c] Department of Transport Technology and Economics, Faculty of Transportation Engineering and Vehicle Engineering, Budapest University of Technology and Economics, 1111 Műegyetem rkp. 3., Budapest, Hungary
[d] Department of Physics, Budapest University of Technology and Economics, 1111 Műegyetem rkp. 3., Budapest, Hungary

ARTICLE INFO

Keywords:
Traffic emission
COPERT
WRF-Chem
Urban air quality
Budapest air quality

ABSTRACT

Due to increasing issues of air pollution in urban areas continuous research is being conducted to upgrade models, which can predict the distribution of pollutants and thus enable timely interventions to mitigate their negative effects. To support these efforts, traffic data from an integrated transport model was used to drive the COPERT traffic emission model and the WRF-Chem atmospheric chemistry model. With reliable macroscopic traffic data from the Budapest region, traffic state estimations were calculated for every fifteen minutes of the day using dynamic assignment with predefined and time-varying static demand matrices. Then the COPERT vehicular emission model of average speeds was applied to provide the emission factors, so that the macroscopic emissions for the traffic network could be calculated. As a next step the WRF-Chem online coupled weather and atmospheric chemistry model was adapted to estimate atmospheric dispersion of pollutants (CO, NO_x, O_3). The coupled models are presented in a 2-day case study with qualitative comparison of obtained results with measurements. As a result, it can be stated that combining macroscopic road traffic modeling with atmospheric models can enhance the estimation efficiency of urban air pollution.

1. Introduction

Traffic-related air pollution has become a serious issue in European cities. Budapest, the capital of Hungary and the 9th largest city of the EU, has been facing high concentrations of particulate matter (PM) and NO_2, which exceed the guidelines defined by the European Environmental Agency. The World Health Organization estimated an approximate 8000 deaths related to outdoor air pollution in Hungary each year (WHO, 2016). While most of the PM_{10} pollution is attributable to domestic heating and large-scale transport, NO_2 is a mainly traffic-related pollutant (Csonka et al., 2020; EEA, 2019; Ferenczi, 2013; Ferenczi and Bozó, 2017; Kis-Kovács et al., 2017). Ozone is a secondary pollutant related to both anthropogenic and biogenic precursors.

Prediction of the air quality for Budapest is performed by the Copernicus Atmospheric Monitoring Service (Marécal et al., 2015)

* Corresponding author.
E-mail address: adam.leelossy@ttk.elte.hu (Á. Leelőssy).

https://doi.org/10.1016/j.uclim.2021.100868
Received 13 November 2020; Received in revised form 12 April 2021; Accepted 28 April 2021
Available online 6 May 2021

and the Hungarian Meteorological Service (Ferenczi et al., 2014). Emission inventories for these models are available on regular grids with $0.1^\circ \times 0.1^\circ$ or 7 km × 7 km horizontal resolution, e.g. the national NECD-IIR and the European TNO-MACC inventory (Kis-Kovács et al., 2017; Kuenen et al., 2014). However, these inventories cannot describe the fine spatial and diurnal variations of urban traffic. To estimate traffic emissions, top-down and bottom-up approaches are used (Guevara et al., 2017; Kuenen et al., 2014; von Schneidemesser et al., 2017). A top-down method uses observed air quality data on monitoring sites and an inverse atmospheric transport model to obtain an emission field without any actual data on the traffic characteristics (Kuik et al., 2018). A bottom-up approach couples a traffic model with the atmospheric transport model and provides an emission inventory based on the macroscopic traffic characteristics (Csikós et al., 2015; Kuik et al., 2018).

Macroscopic road traffic modeling, on the one hand, consists of a graph-based traffic network representation with edges as road links and nodes as intersections. On the other hand, a macroscopic traffic model comprises a good representation of travel demands determined by an appropriate origin-destination matrix, which is practically the first step of the classical road traffic forecasting, i.e. trip generation and trip distribution (de Dios Ortúzar and Willumsen, 2001). Based on these previous steps, mode choice modeling and route assignment can be carried out in order to allocate trips between each origin-destination pair. As an output of the macroscopic model, average traffic volume and traveling speed can be assigned to all road links within the network, based on which total emission of pollutant over a finite spatiotemporal domain can be estimated (Csikós, 2015). Moreover, the estimated emission might be improved with portable emission measurement systems (O'Driscoll et al., 2016).

Besides air quality prediction, coupled traffic and atmospheric modeling can be used to assess the impacts of emission reduction policies (José et al., 2018), for source attribution (Liu et al., 2018), to investigate future scenarios (Saikawa et al., 2011) and to better understand the relationship between traffic characteristics and air quality (Pachón et al., 2018). Coupling traffic and atmospheric models also enable the use of real-time GPS-based traffic data as an input for air quality nowcasting (Ibarra Espinosa et al., 2017). Parallel usage of top-down and bottom-up methods helps to investigate the impact of vehicles with increased emission factor due to bad maintenance or a malicious bypass of emission reduction systems (von Schneidemesser et al., 2017).

In 2015, the mobility manager of Budapest (called Centre for Budapest Transport), has developed an integrated Multimodal Transport Model (MTM) that provides valuable high-resolution simulated road traffic data (Mátrai et al., 2015) which can be further used for emission estimation. However, any application that couples the MTM traffic simulation with an atmospheric transport model is still lacking. In this study, we present a WRF-Chem atmospheric chemistry simulation driven by traffic emissions obtained from the MTM traffic model and the COPERT traffic emission model.

In this study, we show an efficient approach to estimate the air pollution level in Budapest. It is well-known that the course of the concentration of the air pollutants farther (ranging between local and regional scales) from the cities is governed by the cumulative emissions originated from traffic and other sources. However, air quality in the urban environment is very sensitive to the temporal changes of the emission which is mostly originated by the traffic. To address this important issue, our main aim was to develop a model framework coupling an air quality model with a high spatial and temporal resolution traffic emission model and present a case study for this integrative approach.

2. Methods

2.1. Traffic network modeling

For large scale traffic modeling the classical macroscopic approach is straightforward. Hence, the well-known four-step model was applied in order to estimate the urban traffic and related macroscopic emission. In our contribution, we had the opportunity to use reliable macroscopic traffic data of the mobility manager of the Hungarian capital (Mátrai et al., 2015), which data can be freely used for research. The MTM encompasses Budapest area and the entire municipal region which is relevant for commuter transport modeling purposes. Budapest has about 500,000 commuters per day. MTM's four-step model consists of 922 transport modeling zones, 10,700 nodes and 30,000 road links.

Based on the MTM data, a traffic state estimation was calculated for every fifteen minutes of the day by working with a dynamic assignment with predefined and time-varying static demand matrices (Horváth et al., 2017). The MTM transport model applies general working day demand, i.e. for the 2 days simulation the same daily traffic flows were calculated changing with the applied 15-min temporal resolution. By using VISUM traffic modeler, a general business day was simulated providing the two main macroscopic traffic variables concerning all links of the Budapest network, i.e. mean speed and traffic flow.

2.2. Modeling of road traffic emission

Vehicular emission models are developed to characterize gaseous pollution and fuel consumption on a microscopic level. The output of the models is given by the emission factor *ef*, which is the normalized intensity of pollutant emission: usually the distant specific emission in the unit [g/km]. According to the scale of input parameters, a variety of models have been proposed. Modal models, e.g., CMEM and MOVES (Chamberlin et al., 2011) provide the most accurate description of emission by using low-level vehicle operation parameters, i.e., engine speed, gear level, etc. Reducing the number of input parameters, a less accurate description can be obtained by the so-called cycle variable models, e.g., VERSIT (Smit et al., 2007) and VT-Micro (Rakha et al., 2004), which give emission factors as functions of various driving cycle variables (e.g., instantaneous speeds, idle time, acceleration, road slopes). Average speed models, e.g., COPERT (Ntziachristos et al., 2000) and (EMFAC, 2002) use the least number of input parameters, resulting in a low-resolution model. In this case emission factors are given as functions of average traveling speeds of standard driving

cycles.

The current work uses the emission factor of an average-speed emission model for two main reasons. First, the accessible system measurements are constrained to macroscopic variables, accepting flow and speed measurements as the input variable of the average speed model. Second, even though average acceleration can be obtained in a macroscopic sense (Luspay et al., 2010), their values remain low due to the rare spatiotemporal sampling and have a negligible effect on emission values. For a quantitative analysis of the effect of using macroscopic acceleration values in VT-Micro model, the reader is referred to (Csikós et al., 2011). An analysis for the use of average-speed emission modeling with different traffic models is given in (Zhu et al., 2013).

The emission factor function $ef^p(v)$ of the applied average-speed emission model COPERT (Ntziachristos et al., 2000) is given by the equation

$$ef^p(v) = \frac{\alpha^p + \gamma^p v + \varepsilon^p v^2}{1 + \beta^p v + \delta^p v^2} \tag{1}$$

where parameters α^p, β^p, γ^p, δ^p, ε^p of pollutant p are determined by curve fitting to vehicle dynamometer measurements of prespecified driving cycles, and v is the average speed. In the followings, the macroscopic description of traffic emission is summarized. Without the loss of generality, assume that the vehicle composition is homogeneous and constant in time and its emission factor for pollutant p is represented by ef^p. Then, the spatiotemporal distribution of traffic emission e for pollutant p is given as follows in the continuous domain:

$$e^p(x,t) = ef^p(v(x,t)) \cdot q(x,t) \tag{2}$$

where $q(x,t)$ denotes the continuous vehicle flow at location x and time t, obtained by the fundamental equation

$$q(xt) = \rho(xt) \cdot v(xt) \tag{3}$$

Continuous variables $\rho(x,t)$ and $v(x,t)$ denote the traffic density and mean speed, respectively. The variable $e^p(x,t)$ is obtained in unit [veh g/km h]. Total emission of pollutant p in unit [veh g] over a finite spatiotemporal domain $\Delta x \times \Delta t$ is given by the following integral

$$E_{\Delta x \times \Delta t} = \int_{\Delta t} \int_{\Delta x} ef^p(v(x,t)) \cdot q(x,t)\, dx\, dt \tag{4}$$

Accepting that the average speed of traffic flow represents the speed of individual vehicles over a domain $L_i \times T$, this definition can be extended to discrete space and time. For discrete segment i of length L_i in discrete sample step k of duration T, spatiotemporal distribution of emission of pollutant p is given as:

$$e_i^p(k) = ef^p(v_i(k)) \cdot q_i(k) \tag{5}$$

whereas the total emission in the spatiotemporal rectangle $L_i \times T$ of the discrete measurement can be approximated as

$$E_i^p(k) = ef^p(v_i(k)) \cdot q_i(k) \cdot L_i \cdot \mathrm{T} \tag{6}$$

Based on the traffic data generated by MTM, macroscopic emission was calculated for the Budapest traffic network using the

Table 1
COPERT model parameters.

Parameter	Value
T	0.25 h
L_i	$\in$[0.062; 26.688] km
α^{CO}	1.5778 g/km
β^{CO}	0
γ^{CO}	-0.022 g h/km^2
δ^{CO}	0
ε^{CO}	1.94 10^{-4} g h^2/km^3
α^{HC}	0.1666 g/km
β^{HC}	0
γ^{HC}	-0.017 g h/km^2
δ^{HC}	0
ε^{HC}	2.36 10^{-5} g h^2/km^3
α^{CO_2}	195.3307 g/km
β^{CO_2}	0
γ^{CO_2}	-1.8194 g h/km^2
δ^{CO_2}	0
ε^{CO_2}	0.0247 g h^2/km^3
α^{NO_x}	0.8162 g/km
β^{NO_x}	0
γ^{NO_x}	-0.097 g h/km^2
δ^{NO_x}	0
ε^{NO_x}	1.49 10^{-4} g h^2/km^3

COPERT emission model. Link-level traffic emission was calculated from (6) with a constant sampling time T and link-dependent L_i. The emission values for pollutants CO, HC (total hydrocarbons) and NO_x were calculated according to the emission model coefficients and sampling constants given in Table 1.

Obtained pollution masses were aggregated on a 1 km × 1 km grid to provide input data for the atmospheric model. This was performed by regarding each link as a series of equidistant point sources located 10 m after one another along the line. The link emission is split equally among the corresponding point sources, and then the total emission of a grid cell is given as the sum of point sources that fall within the given cell.

2.3. Dispersion model

Atmospheric dispersion of pollutants was simulated with the WRF-Chem v3.6 online coupled atmospheric chemistry transport model (Grell et al., 2005) adapted for the simulation of air quality in Hungary (Kovács et al., 2019). WRF-Chem is one of the most widely used mesoscale model for weather and air quality prediction, and has been successfully coupled with traffic emission models in several applications (Ibarra Espinosa et al., 2017; José et al., 2018; Liu et al., 2018; von Schneidemesser et al., 2017; Vara-Vela et al., 2016).

Numerical weather simulations in WRF-Chem were performed using three nested domains (Fig. 1) with 40 vertical levels for meteorology and the lowest 10 levels for chemistry simulation. The external domain had a size of 1500 km × 1050 km with horizontal resolution of 15 km. The middle domain covered Hungary with a 5 km grid, while the internal domain was a 105 km × 105 km square containing Budapest and its surroundings with horizontal resolution of 1 km. Meteorological boundary conditions were provided by the GFS (Global Forecast System) model with 0.25 degree horizontal and 3-h temporal resolutions (NOAA, 2016). As the research aimed to study the traffic-related pollutants, no emission inventory was applied other than that simulated by the MTM-COPERT model described in Sections 2.1–2.2. Chemical initial conditions were given by a 1-day spin-up period, initiated from a homogenous background concentration of CO, NO_x and O_3 values defined as the mean concentration over monitoring sites in Budapest at 0 UTC 25 September 2018, the start time of the spin-up day. For the chemistry simulation, the RADM2 chemical mechanism was applied with the KPP kinetic pre-processor (Stockwell et al., 1990). The list of applied parameterization schemes is given in Table 2.

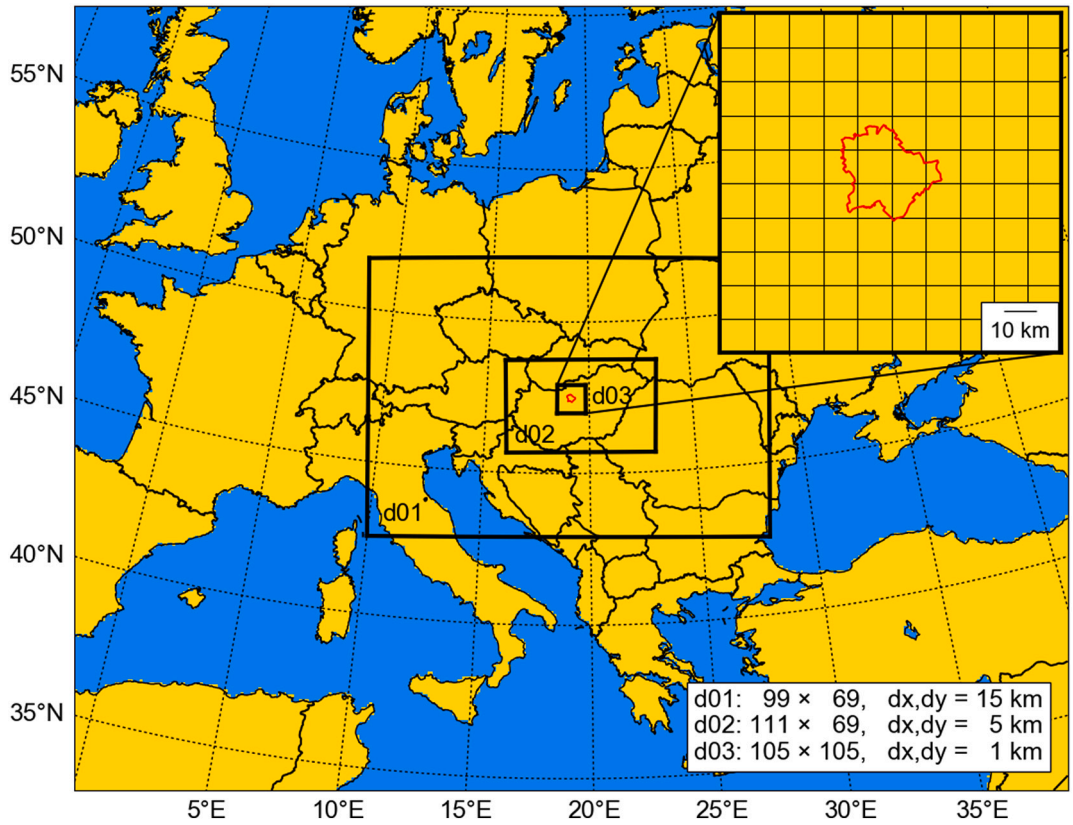

Fig. 1. WRF-Chem model domains: d01, d02 and d03 domains have 15, 5 and 1 km spatial resolution, respectively. Domain d03 covers Budapest and its surroundings.

Table 2
WRF-Chem parameterizations.

Physical/chemical process	Applied scheme
Planetary boundary layer	Mellor–Yamada–Janjic scheme
Microphysics	WRF Single-Moment 6-class scheme
Photolysis	Fast-J photolysis
Gas-phase chemistry	Regional Acid Deposition Model 2
Longwave radiation	Rapid Radiative Transfer Model
Shortwave radiation	Old Goddard scheme
Cumulus convection	Grell–Freitas ensemble scheme
Urban canopy	Building Environment Parameterization
Land surface process	Noah Land Surface Model
Surface layer scheme	Monin–Obukhov–Janjic Eta similarity scheme

2.4. The case study

To demonstrate the model in a case study, a period was selected when the impact of traffic-related emissions is assumed to be the strongest compared to other factors determining the air quality of Budapest (Karamchandani et al., 2017) (i.e., domestic heating, large-scale transport, weather). 26–27 September 2016 was selected as the study period. These workdays had calm anticyclonic weather and very weak (< 2 m/s) winds that minimized the weather-related uncertainty and the impact of large-scale transport on air pollution. The clear sky and warm weather (20–21 °C peak temperatures) eliminated domestic heating sources and supported the NO_x-O_3 photochemistry, simulated by the WRF-Chem model. While quantitative validation is not possible due to the unknown urban

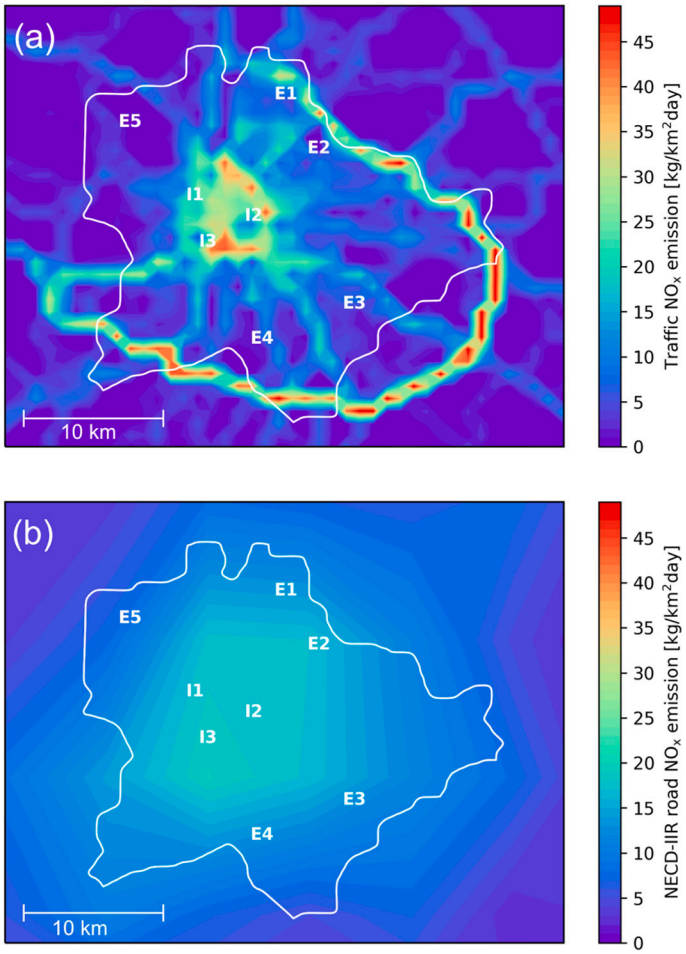

Fig. 2. 24-h NO_x emission of road traffic in Budapest based on the (a) MTM-COPERT model summarized on a 1 km × 1 km grid. (b) NECD-IIR reference inventory of the Hungarian Meteorological Service (Kis-Kovács et al., 2017, p.) (interpolated to the same grid). The administrative boundary of Budapest is shown with a white line. Labels depict the locations and identifiers of air quality monitoring sites.

background pollution and non-traffic emissions, the selected period was suitable to investigate the temporal and spatial pattern of concentrations caused by the coupled effect of commutation and NO_x-O_3 photochemistry, a typical air pollution scenario in summer season anticyclones.

Hourly NO_x, O_3 and CO measurement data were obtained from 8 automatic monitoring sites of the Hungarian Air Quality Network (http://www.levegominoseg.hu/). Monitoring sites have been organized into an internal (I1-I3) and an external (E1-E5) circle to represent the city center and the outer residential ring, respectively (Fig. 2). The initial background concentration was defined as the mean concentration measured at the 8 monitoring sites of Budapest at the start of the spin-up period: 0 UTC, 25 September.

3. Results

3.1. Traffic emissions

Traffic-related CO, NO_x and HC (total hydrocarbons) emissions were calculated based on the MTM-COPERT simulation. Total CO, NO_x and HC emissions in the presented area (Fig. 2) were found to be 11.1, 9.3 and 1.8 t/day, respectively. The spatial distribution of the emission clearly shows the ringed structure of the road network (Fig. 2a). In the city center and at the M0 highway ring near the city border, NO_x emission rate reaches 50–70 kg/km^{2}day. Commuter traffic in the suburbs causes a NO_x emission of 20–30 kg/km^{2}day along the main radial routes. The diurnal variability of emission shows a daytime plateau and nighttime minimum (Fig. 3.). The time of the peak 1-h emission rate over the entire domain is at 2 PM local time, however, the time of NO_x emission peaks varies among different urban sites between 12 and 22 PM (Fig. 3.). A quickly increasing traffic emission is observable in the morning, followed by a plateau of dense traffic until the evening hours.

The obtained emission values can be compared to the National Emission Ceiling Directive Informative Inventory Report (NECD-IIR), the annual emission inventory of Budapest created by the Hungarian Meteorological Service on a 0.1° × 0.1° grid and widely used in environmental applications and international data exchange (Kis-Kovács et al., 2017). The average daily NO_x emission of road transport based on the NECD-IIR dataset is presented in Fig. 2b. The total emission in the presented area is estimated by the NECD-IIR report as 27.4, 14.8 and 4.3 t/day for CO, NO_x and HC, respectively. In comparison with our MTM-COPERT model, NECD-IIR provides higher emission values with a factor of 1.6–2.5. Meanwhile, the peak emission density in the MTM-COPERT model was 65.6, 69.9 and 11.8 kg/km^{2}day, while NECD-IIR yielded 35.3, 19.1 and 5.6 kg/km^{2}day for CO, NO_x and HC, respectively. Despite the relatively fine (0.1°) resolution of the NECD-IIR dataset, it only provides a concentric emission peak in the city, while the radial commutation routes and the M0 highway ring are undetectable (Fig. 2b.). Therefore, while the MTM-COPERT simulation provides a lower overall emission estimate, it brings major improvement in the representation of emission hotspots, especially in the suburban areas.

A possible cause of the overall underestimation in the MTM-COPERT model is the presence of transit traffic flow, as no demand matrices are available for the simulation of long-range (national and international) travel routes crossing Budapest. As a great advantage compared to NECD-IIR, the MTM-COPERT traffic emission simulation provides fine spatial and temporal details of the emission that can be applied to investigate the urban-scale and diurnal pattern of traffic-related air pollution in the city.

3.2. Atmospheric concentrations

Fig. 4. shows the simulated morning (8 AM local time) and evening (8 PM local time) concentrations of NO_x and O_3. The spatial structure of the NO_x field follows closely the traffic density. However, calm wind allows the NO_x emission from several hours of high

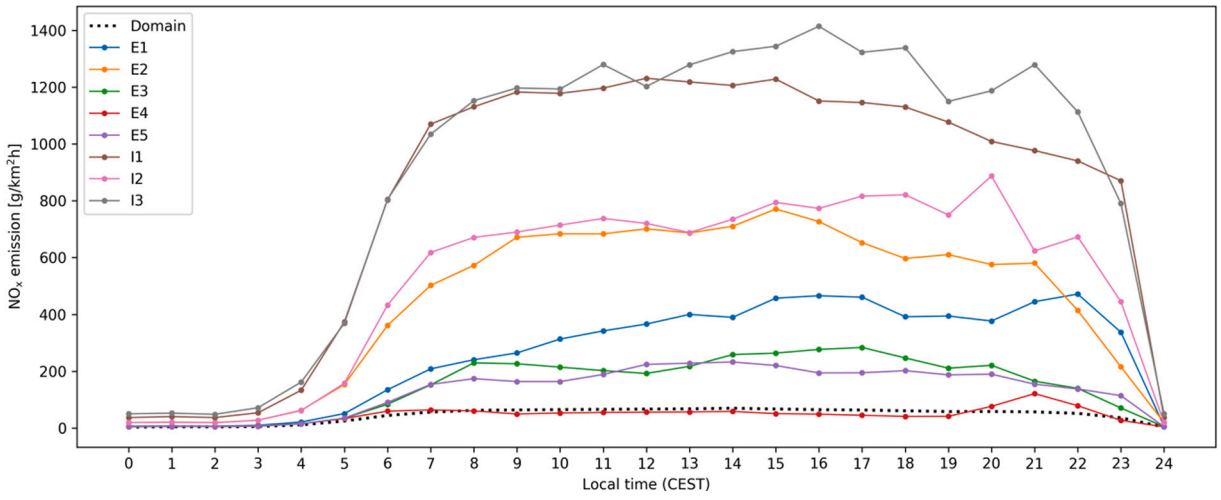

Fig. 3. Diurnal variability of traffic-related NO_x emission based on the MTM-COPERT model. Colored lines show the hourly emission rates in the 1 km × 1 km grid cells of the respective monitoring sites. Black dotted line shows the mean NO_x emission rate in the 105 × 105 km model domain.

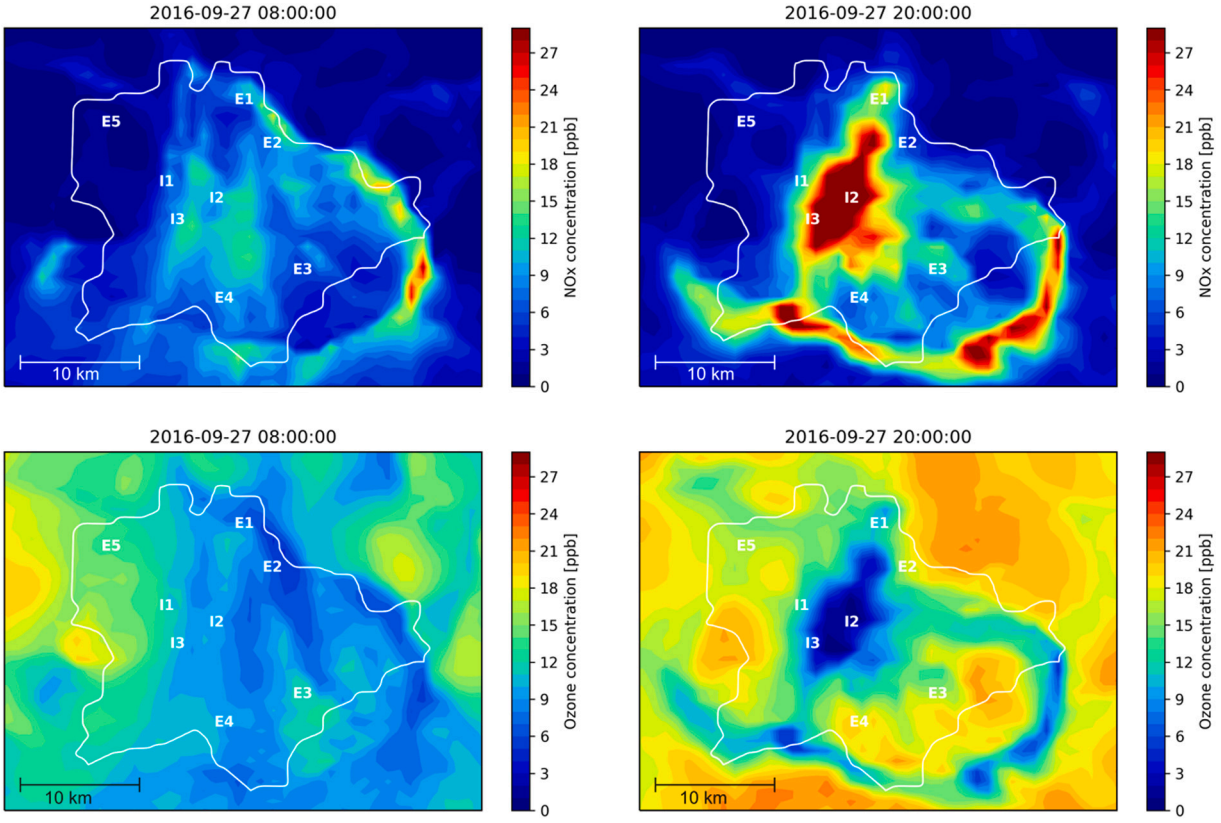

Fig. 4. Simulated NO_x (upper row) and O_3 (lower row) concentrations at 6 and 18 UTC (8 AM and 8 PM local time in the left and right columns, respectively), 27 September 2016. The afternoon ozone peak and the inverse relationship between NO_x and O_3 is well observable.

traffic during the afternoon to accumulate in the urban air. Therefore, evening concentrations were simulated to be higher than those in the morning rush hours, and the maximum NO_x concentrations were found in the late evening hours (8–11 PM local time).

Ozone concentrations show a clear daytime and afternoon maximum, while concentrations are low in the morning hours. The inverse relationship between NO_x and O_3 concentrations is explained by the fact that direct NO emission decays ozone. Highest ozone concentrations are found in the southern and eastern suburbs, and mainly in the agglomeration out of the city borders. However, the two areas are clearly divided by a significant feature of the urban structure, the M0 highway ring, that largely reduces O_3 and increases NO_x pollution in a 1–2 km wide band.

A similar effect with a smaller amplitude is observable in the striped structure of the air pollution of the southeastern suburbs. While this is the main place of ozone production from the nitrogen oxides transported from the city center, the radial commuter routes also represent a significant local NO_x source. This results in radial bands of high-NO_x and low-O_3 areas depicting high-traffic roads in a low-NO_x and high-O_3 environment (Fig. 4).

Simulated concentrations were compared to measurements at the I3 and E3 monitoring sites (Fig. 5). Site I3 is located at Kosztolányi square (Budapest), a congested junction of two 2 × 2 lane roads, both of which are important commuter routes. The sampling point is divided from the junction with an only 50 m wide green area. As the local traffic is very dense, and no other significant air pollution sources are in the vicinity, NO_x air pollution measured at station I3 is assumed to be largely attributable to road traffic. The MTM-COPERT traffic emission simulation also showed the highest local NO_x emission among the urban monitoring sites (Fig. 3.).

Observed NO_x concentrations presented in Fig. 5 show the typical two-peak behavior, peaking at 8–9 AM and 7–10 PM local time. A similar temporal pattern is simulated in the WRF-Chem model, although the NO_x concentrations and the peak amplitudes are seriously underestimated.

Concentration timelines were also compared at station E3, an urban background monitoring site at Gilice square (Budapest) in the southeastern suburbs. E3 lies in the suburban ozone maximum area, thus the measurements should represent the behavior of urban ozone photochemistry. Although the local area is not affected by heavy traffic, the two-peak NO_x timeline is present with a smaller amplitude than at station I3. However, the NO_x concentrations are still seriously underestimated.

4. Discussion

Diurnal variability of near-road air pollution is defined by the interaction of traffic density, atmospheric chemistry and vertical

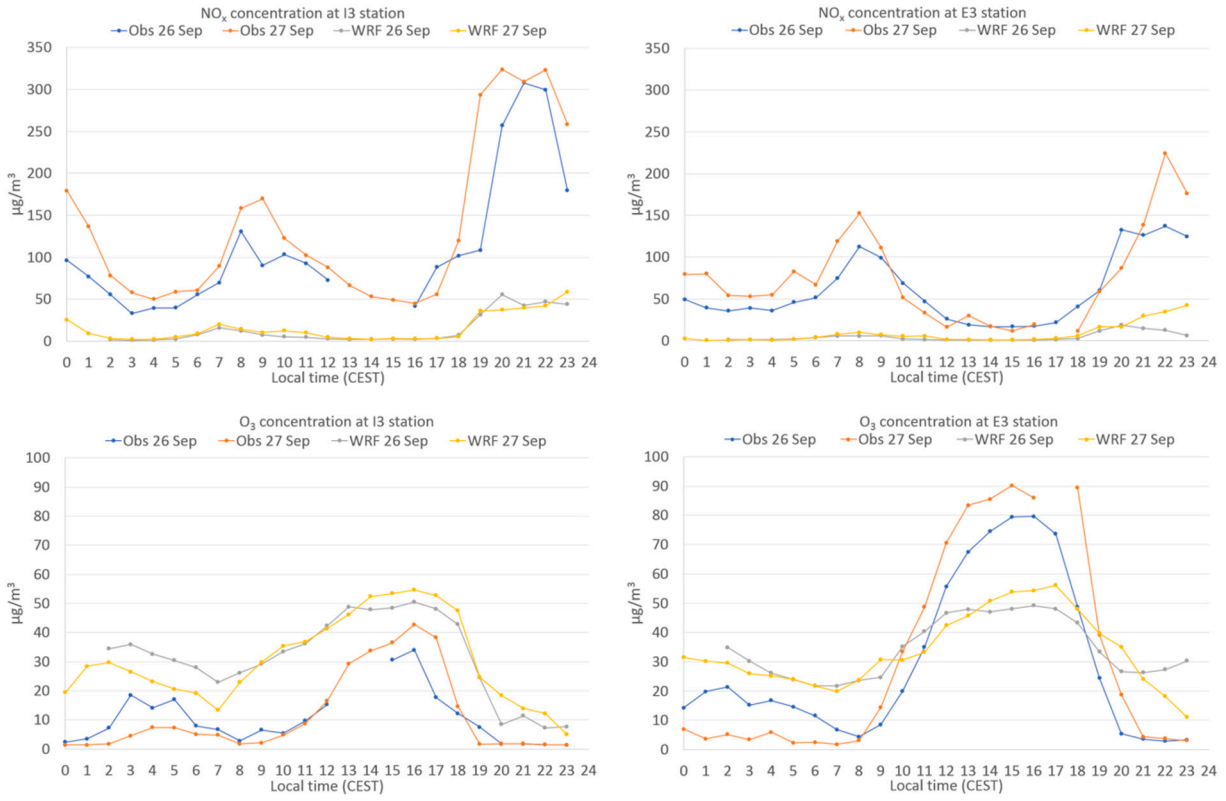

Fig. 5. Comparison of observed and simulated diurnal cycles of NO_x and O_3 concentration at an urban (I3) and suburban (E3) station.

mixing. Coupling a traffic emission model with an atmospheric chemistry and transport model can represent these processes. In a fair-weather case study, the fine-scale spatial and diurnal patterns of NO_x and O_3 concentrations were investigated.

An important observation is that the two-peak NO_x timeline appears in the simulated NO_x concentrations, although it is not present in the simulated traffic density, and thus the NO_x emission timeline (Figs. 2 and 5). Therefore, the two-peak NO_x behavior is not necessarily a marker of the morning and afternoon rush hours' traffic, but rather the interaction of traffic, meteorological and chemical processes. In the first 1–2 h after sunrise, the traffic density, the ozone production and the PBL height are all relatively low, though rapidly increasing. After 9 AM, convective mixing and the initiation of ozone production explains the decrease of NO_x concentrations despite the further increasing emission rate. The simulated NO_x peak is in the late evening, between 7 and 10 PM, in agreement with the measurements. The highest traffic emission rate is simulated to be a few hours earlier (between 3 and 6 PM, Fig. 3.). The NO_x concentration peak is delayed until sunset when photochemical ozone production and efficient vertical mixing halts. Sunrise and sunset on these days were at 6:37 AM and 6:30 PM, respectively. Ozone shows the inverse temporal trend of NO_x.

The model seriously underestimated the NO_x concentrations and also the diurnal amplitude of NO_x variability, which is clearly related to local traffic emissions. The reason behind this might be the ignorance of transiting traffic, the underestimation of emission factors or the traffic density. The selection of the chemical mechanism in the WRF-Chem model is another factor of uncertainty (Kovács et al., 2019; Mar et al., 2016). However, this error leads to an important observation regarding potential emission reduction measures. The low simulated NO_x concentrations caused an overestimation of ozone values in the urban site, but underestimation of ozone values in the suburban site. As the local NO_x emission is low near the E3 suburban station, ozone production is based on the precursors transported from the city center located 5–15 km to the northwest, or from the M0 highway located 8–10 km to the south, depending on the wind direction. The general underestimation of NO_x levels means less precursor for ozone production in suburban afternoons, while it causes less NO for ozone decay in the city center and at night. It should be noted that the underestimation of NO_x is in the urban environment is a usual feature observed in model simulations. For instance, in a very recent work of Veratti et al. (2020), the authors highly underestimated the concentration of NO_x in Modena (Italy) when they modeled it with the WRF-Chem. To improve the model performance, they extended the model system with a micro-scale Lagrangian approach.

It must be noted here that our simulation only demonstrates the complex behavior of traffic-related urban air pollution in a simple case study. To generalize this model for operational use, a detailed large-scale inventory of other precursors, such as biogenic VOCs, domestic CO and industrial NO_x must be considered to provide an accurate simulation of large-scale transport and the chemical interaction of local and non-local air pollution.

5. Conclusions

A coupled simulation of traffic network, traffic emission, atmospheric transport and atmospheric chemistry has been presented in an urban case study, representing a typical weekday scenario in an early autumn anticyclone. This is the first application that couples Budapest's Multimodal Transport Model, provided by the mobility manager of Budapest, the COPERT traffic emission model and the WRF-Chem atmospheric chemistry and transport model. This new coupling allows the study of the diurnal and urban-scale spatial characteristic of traffic-related air pollution in Budapest, which was not possible with existing emission inventories. In this study, we focused on the precise modeling of traffic-related emission in high spatial and time resolutions because in other studies on the urban scale the results of the model simulation suggested that contribution to the atmospheric NO_x level originated from the domestic heating or industrial combustion are not as relevant as the traffic-related emission (Ghermandi et al., 2020). WRF-Chem model has been mostly used in regional scale of air pollution modeling utilizing its feature, namely, it is an Eulerian model based on solving of atmospheric transport equations on computational meshes (Kuik et al., 2016; Sharma et al., 2016; Veratti et al., 2020). This approach provides an optimal balance between the resolution of the domain and domain size. An Eulerian model can capture the long-term spatiotemporal evolution of the air pollution levels at a greater domain than the local scale. However, when local effects in urban area arising from the high variability of either meteorological or emission data may provide high uncertainties in the simulation results. To address this challenging issue, additional efforts should be performed (Veratti et al., 2020).

Traffic-related emissions were simulated with 15-min temporal resolution at each node of the urban and suburban road network using traffic characteristics and COPERT emission factors. The temporal and spatial pattern of traffic-related NO_x and O_3 air pollution were modeled with the WRF-Chem online coupled atmospheric chemistry model. The traffic simulation yielded a nearly uniform, high traffic density throughout the day with a rapid increase in the morning hours and decrease in the late evening. Meanwhile, a morning and afternoon two-peak NO_x timeline was found in both the measured and the simulated air quality time series. Therefore, the two-peak behavior of NO_x is attributable to atmospheric processes as well as the traffic characteristics. The simulated diurnal patterns agree with measurements, but NO_x concentrations are seriously underestimated. Underestimation of NO_x concentrations resulted in an overestimation of urban, but an underestimation of suburban ozone levels. Our main aim was to develop a framework coupling an air quality model with a traffic emission model to serve as a basis for further investigation of air quality in urban environments in Budapest and similar-sized cities. Future work will incorporate the emissions from transit traffic flow in the model and use updated emission factors to better represent real-life scenarios.

Declaration of Competing Interest

Authors declare no conflict of interest.

Acknowledgement

The research reported in this paper and carried out at BME has been supported by the NRDI Fund (TKP2020 IES, Grant No. BME-IE-MIFM) based on the charter of bolster issued by the NRDI Office under the auspices of the Ministry for Innovation and Technology. The research was funded by the National Research, Development and Innovation Office of Hungary (Nos. K116506, K128805-K128818).

References

Chamberlin, R., Swanson, B., Talbot, E., Dumont, J., Pesci, S., 2011. Analysis of MOVES and CMEM for evaluating the emissions impact of an intersection control change. In: Presented at the Transportation Research Board 90th Annual Meeting, Washington DC, USA.

Csikós, A., 2015. Modeling and Control Methods for the Reduction of Traffic Pollution and Traffic Stabilization (PhD thesis). Budapest University of Technology and Economics, Budapest.

Csikós, A., Luspay, T., Varga, I., 2011. Modeling and optimal control of travel times and traffic emission on freeways. In: IFAC Proc. Vol., 18th IFAC World Congress 44, pp. 13058–13063. https://doi.org/10.3182/20110828-6-IT-1002.01958.

Csikós, A., Tettamanti, T., Varga, I., 2015. Macroscopic modeling and control of emission in urban road traffic networks. Transport 30, 152–161. https://doi.org/10.3846/16484142.2015.1046137.

Csonka, B., Havas, M., Csiszár, C., Földes, D., 2020. Operational methods for charging of electric vehicles. Period. Polytech. Transp. Eng. 48, 369–376. https://doi.org/10.3311/PPtr.15853.

de Dios Ortúzar, J., Willumsen, L.G., 2001. Modelling Transport. Wiley.

EEA, 2019. Air Quality in Europe - 2019 Report (No. EEA reports No. 10/2019). European Environment Agency, Copenhagen.

EMFAC, 2002. Technical Report. California Air Resources Board (CARB) Emission Inventory Series.

Ferenczi, Z., 2013. Predictability analysis of the PM2.5 and PM10 concentration in Budapest. Időjárás 117, 359–375.

Ferenczi, Z., Bozó, L., 2017. Effect of the long-range transport on the air quality of greater Budapest area. Int. J. Environ. Pollut. 62, 407–416. https://doi.org/10.1504/IJEP.2017.089428.

Ferenczi, Z., Labancz, K., Steib, R., 2014. Development of a numerical prediction model system for the assessment of the air quality in Budapest. In: Steyn, D., Mathur, R. (Eds.), Air Pollution Modeling and Its Application XXIII, Springer Proceedings in Complexity. Springer International Publishing, pp. 401–405.

Ghermandi, G., Fabbi, S., Veratti, G., Bigi, A., Teggi, S., 2020. Estimate of secondary NO2 levels at two urban traffic sites using observations and modelling. Sustainability 12, 7897. https://doi.org/10.3390/su12197897.

Grell, G.A., Peckham, S.E., Schmitz, R., McKeen, S.A., Frost, G., Skamarock, W.C., Eder, B., 2005. Fully coupled "online" chemistry within the WRF model. Atmos. Environ. 39, 6957–6975. https://doi.org/10.1016/j.atmosenv.2005.04.027.

Guevara, M., Lopez-Aparicio, S., Cuvelier, C., Tarrason, L., Clappier, A., Thunis, P., 2017. A benchmarking tool to screen and compare bottom-up and top-down atmospheric emission inventories. Air Qual. Atmos. Health 10, 627–642. https://doi.org/10.1007/s11869-016-0456-6.

Horváth, M.T., Mátrai, T., Tóth, J., 2017. Route planning methodology with four-step model and dynamic assignments. Transp. Res. Procedia 27, 1017–1025. https://doi.org/10.1016/j.trpro.2017.12.127.

Ibarra Espinosa, S., Ynoue, R., Giannotti, M., 2017. Integrating internet GPS vehicle tracking data into a bottom-up vehicular emissions inventory and atmospheric simulation in South-East, Brazil. In: AGU Fall Meet. Abstr. 43.

José, R.S., Pérez, J.L., Pérez, L., Barras, R.M.G., 2018. Using the WRF-Chem model to evaluate urban emission reduction strategies - Madrid case study. LIFE Int. J. Health Life-Sci. 4.

Karamchandani, P., Long, Y., Pirovano, G., Balzarini, A., Yarwood, G., 2017. Source-sector contributions to European ozone and fine PM in 2010 using AQMEII modeling data. Atmos. Chem. Phys. 17, 5643–5664. https://doi.org/10.5194/acp-17-5643-2017.

Kis-Kovács, G., Tarczay, K., Kőbányai, K., Ludányi, E., Nagy, E., Lovas, K., 2017. Informative Inventory Report 1990–2015. Hungarian Meteorological Service, Unit of National Emissions Inventories, Budapest.

Kovács, A., Leelőssy, Á., Mészáros, R., Lagzi, I., 2019. Online coupled modelling of weather and air quality of Budapest using the WRF-Chem model. Időjárás 123, 203–215.

Kuenen, J.J.P., Visschedijk, A.J.H., Jozwicka, M., Denier van der Gon, H.A.C., 2014. TNO-MACC_II emission inventory; a multi-year (2003–2009) consistent high-resolution European emission inventory for air quality modelling. Atmos. Chem. Phys. 14, 10963–10976. https://doi.org/10.5194/acp-14-10963-2014.

Kuik, F., Lauer, A., Churkina, G., Denier van der Gon, H.A.C., Fenner, D., Mar, K.A., Butler, T.M., 2016. Air quality modelling in the Berlin–Brandenburg region using WRF-Chem v3.7.1: sensitivity to resolution of model grid and input data. Geosci. Model Dev. 9, 4339–4363. https://doi.org/10.5194/gmd-9-4339-2016.

Kuik, F., Kerschbaumer, A., Lauer, A., Lupascu, A., von Schneidemesser, E., Butler, T.M., 2018. Top–down quantification of NO_x emissions from traffic in an urban area using a high-resolution regional atmospheric chemistry model. Atmos. Chem. Phys. 18, 8203–8225. https://doi.org/10.5194/acp-18-8203-2018.

Liu, Y.-H., Ma, J.-L., Li, L., Lin, X.-F., Xu, W.-J., Ding, H., 2018. A high temporal-spatial vehicle emission inventory based on detailed hourly traffic data in a medium-sized city of China. Environ. Pollut. 236, 324–333. https://doi.org/10.1016/j.envpol.2018.01.068.

Luspay, T., Kulcsar, B., Varga, I., Zegeye, S.K., De Schutter, B., Verhaegen, M., 2010. On acceleration of traffic flow. In: Presented at the 13th International IEEE Conference on Intelligent Transportation Systems, IEEE, Funchal, Madeira Island, Portugal, pp. 741–746. https://doi.org/10.1109/ITSC.2010.5625204.

Mar, K.A., Ojha, N., Pozzer, A., Butler, T.M., 2016. Ozone air quality simulations with WRF-Chem (v3.5.1) over Europe: model evaluation and chemical mechanism comparison. Geosci. Model Dev. 9, 3699–3728. https://doi.org/10.5194/gmd-9-3699-2016.

Marécal, V., Peuch, V.-H., Andersson, C., Andersson, S., Arteta, J., Beekmann, M., Benedictow, A., Bergström, R., Bessagnet, B., Cansado, A., Chéroux, F., Colette, A., Coman, A., Curier, R.L., Denier van der Gon, H.A.C., Drouin, A., Elbern, H., Emili, E., Engelen, R.J., Eskes, H.J., Foret, G., Friese, E., Gauss, M., Giannaros, C., Guth, J., Joly, M., Jaumouillé, E., Josse, B., Kadygrov, N., Kaiser, J.W., Krajsek, K., Kuenen, J., Kumar, U., Liora, N., Lopez, E., Malherbe, L., Martinez, I., Melas, D., Meleux, F., Menut, L., Moinat, P., Morales, T., Parmentier, J., Piacentini, A., Plu, M., Poupkou, A., Queguiner, S., Robertson, L., Rouïl, L., Schaap, M., Segers, A., Sofiev, M., Tarasson, L., Thomas, M., Timmermans, R., Valdebenito, Á., van Velthoven, P., van Versendaal, R., Vira, J., Ung, A., 2015. A regional air quality forecasting system over Europe: the MACC-II daily ensemble production. Geosci. Model Dev. 8, 2777–2813. https://doi.org/10.5194/gmd-8-2777-2015.

Mátrai, T., Ábel, M., Kerényi, L.S., 2015. How can a transport model be integrated to the strategic transport planning approach: A case study from Budapest. In: Presented at the International Conference on Models and Technologies for Intelligent Transportation Systems, IEEE, Budapest, Hungary, pp. 192–199. https://doi.org/10.1109/MTITS.2015.7223256.

NOAA, 2016. NCEP GDAS/GFS Global Tropospheric Analyses and Forecast Grids [WWW Document]. http://www.emc.ncep.noaa.gov/GFS/ (Accessed 10.13.16).

Ntziachristos, L., Samaras, Z., Eggleston, S., Gorissen, S., Hassel, D., Hickman, A., Joumard, R., Rijkeboer, R., White, L., Zierock, K., 2000. COPERT III Computer Programme to Calculate Emissions from Road Transport - Methodology and Emission Factors (Version 2.1) (Technical Report No. 49). European Environmental Agency, Copenhagen.

O'Driscoll, R., ApSimon, H.M., Oxley, T., Molden, N., Stettler, M.E.J., Thiyagarajah, A., 2016. A Portable Emissions Measurement System (PEMS) study of NOx and primary NO2 emissions from Euro 6 diesel passenger cars and comparison with COPERT emission factors. Atmos. Environ. 145, 81–91. https://doi.org/10.1016/j.atmosenv.2016.09.021.

Pachón, J., Galvis, B., Lombana, O., Carmona, L., Fajardo, S., Rincón, A., Meneses, S., Chaparro, R., Nedbor-Gross, R., Henderson, B., Pachón, J.E., Galvis, B., Lombana, O., Carmona, L.G., Fajardo, S., Rincón, A., Meneses, S., Chaparro, R., Nedbor-Gross, R., Henderson, B., 2018. Development and evaluation of a comprehensive atmospheric emission inventory for air quality modeling in the megacity of Bogotá. Atmosphere 9, 49. https://doi.org/10.3390/atmos9020049.

Rakha, H., Ahn, K., Trani, A., 2004. Development of VT-Micro model for estimating hot stabilized light duty vehicle and truck emissions. Transp. Res. Part Transp. Environ. 9, 49–74. https://doi.org/10.1016/S1361-9209(03)00054-3.

Saikawa, E., Kurokawa, J., Takigawa, M., Borken-Kleefeld, J., Mauzerall, D.L., Horowitz, L.W., O'Hara, T., 2011. The impact of China's vehicle emissions on regional air quality in 2000 and 2020: a scenario analysis. Atmos. Chem. Phys. 11, 9465–9484.

Sharma, S., Chatani, S., Mahtta, R., Goel, A., Kumar, A., 2016. Sensitivity analysis of ground level ozone in India using WRF-CMAQ models. Atmos. Environ. 131, 29–40. https://doi.org/10.1016/j.atmosenv.2016.01.036.

Smit, R., Smokers, R., Rabé, E., 2007. A new modelling approach for road traffic emissions: VERSIT+. Transp. Res. Part Transp. Environ. 12, 414–422. https://doi.org/10.1016/j.trd.2007.05.001.

Stockwell, W.R., Middleton, P., Chang, J.S., Xiaoyan, T., 1990. The second generation regional acid deposition model chemical mechanism for regional air quality modeling. J. Geophys. Res. Atmos. 95, 16343–16367. https://doi.org/10.1029/JD095iD10p16343.

Vara-Vela, A., Andrade, M.F., Kumar, P., Ynoue, R.Y., Muñoz, A.G., 2016. Impact of vehicular emissions on the formation of fine particles in the Sao Paulo Metropolitan Area: a numerical study with the WRF-Chem model. Atmos. Chem. Phys. 16, 777–797. https://doi.org/10.5194/acp-16-777-2016.

Veratti, G., Fabbi, S., Bigi, A., Lupascu, A., Tinarelli, G., Teggi, S., Brusasca, G., Butler, T.M., Ghermandi, G., 2020. Towards the coupling of a chemical transport model with a micro-scale Lagrangian modelling system for evaluation of urban NOx levels in a European hotspot. Atmos. Environ. 223, 117285. https://doi.org/10.1016/j.atmosenv.2020.117285.

von Schneidemesser, E., Kuik, F., Mar, K.A., Butler, T., 2017. Potential reductions in ambient NO 2 concentrations from meeting diesel vehicle emissions standards. Environ. Res. Lett. 12, 114025. https://doi.org/10.1088/1748-9326/aa8c84.

WHO, 2016. Ambient Air Pollution: A Global Assessment of Exposure and Burden of Disease. World Health Organization, Geneva, Switzerland.

Zhu, F., Lo, H.K., Lin, H.-Z., 2013. Delay and emissions modelling for signalised intersections. Transp. B Transp. Dyn. 1, 111–135. https://doi.org/10.1080/21680566.2013.821689.